Template-Free Hydrothermal Synthesis and Luminescent Properties of Octahedral NaGd?(?MoO $_4$?)?$_2$?:?Eu$^{3?+?}$ Microcrystals

Wangda Gong, Zuoling Fu, Shihong Zhou, Shan Du, Siyuan Zhang, Zhenwen Dai and Wenhao Li

J. Electrochem. Soc. 2010, Volume 157, Issue 10, Pages J338-J341.
doi: 10.1149/1.3467792

Journal of The Electrochemical Society, **157** (10) J338-J341 (2010)
0013-4651/2010/157(10)/J338/4/$28.00 © The Electrochemical Society

Template-Free Hydrothermal Synthesis and Luminescent Properties of Octahedral $NaGd(MoO_4)_2:Eu^{3+}$ Microcrystals

Wangda Gong,[a] Zuoling Fu,[a,b,z] Shihong Zhou,[c] Shan Du,[a] Siyuan Zhang,[c] Zhenwen Dai,[a,b,z] and Wenhao Li[d]

[a]*Key Laboratory of Coherent Light, Atomic and Molecular Spectroscopy, Ministry of Education, College of Physics, Jilin University, Changchun 130023, China*
[b]*State Key Laboratory of Superhard Materials, Jilin University, Changchun 130021, China*
[c]*State Key Laboratory of Rare Earth Resources Utilization, Changchun Institute of Applied Chemistry, Chinese Academy of Sciences, Changchun 130022, China*
[d]*Changchun Institute of Optics, Fine Mechanics and Physics, Chinese Academy of Sciences, Changchun 130033, China*

Uniform and well-crystallized octahedral $NaGd(MoO_4)_2:Eu^{3+}$ microcrystals have been successfully synthesized by a facile one-step hydrothermal synthesis method without involving any templates. The prepared samples were systematically characterized by powder X-ray diffraction, field-emission-scanning electron microscopy, photoluminescence (PL), and photoluminescent excitation spectra. The starting pH value played an important role in the pure-phase formation and uniform morphology of octahedral microcrystals. Detailed proofs indicated that the growth process of $NaGd(MoO_4)_2:Eu^{3+}$ microcrystals was dominated by a nucleation–crystallization-oriented attachment mechanism. Furthermore, the luminescent properties of the as-synthesized $NaGd(MoO_4)_2:Eu^{3+}$ microcrystals were investigated, demonstrating that the PL intensity was influenced by the different morphologies, and the bipyramidal octahedra $NaGd(MoO_4)_2:Eu^{3+}$ luminescent microcrystals might be applied as an excellent red component for near-UV white light emitting diodes.
 [DOI: 10.1149/1.3467792]

Manuscript submitted May 19, 2010; revised manuscript received June 25, 2010. Published August 12, 2010.

The synthesis of micro- and nanoscale inorganic materials with special size, morphology, and hierarchy has stimulated intensive interest because of their importance in basic scientific research and potential technological applications of such materials.[1-3] Many recent efforts have been devoted to the morphological control and spatial patterning of various materials, which is a crucial step toward the realization of functional nanosystems.[4-7] Among various methods used, such as chemical vapor deposition methods or solution-phase chemical routes, they usually require catalysts, expensive and even toxic templates or surfactants, high temperature, and series of complicated procedures. Therefore, it is still a big challenge to develop simple and reliable synthetic methods for hierarchical architectures with designed chemical components and controlled morphologies, which strongly affect the properties of nano/micromaterials.

Metal molybdates have a high application potential in various fields such as photoluminescence (PL), microwave applications, optical fibers, scintillator materials, humidity sensors, and catalysis.[8-11] Lately, more and more attention is paid to red-emitting phosphor based on Eu^{3+}-doped molybdates used for white light emitting diodes (LEDs) because of their intense charge-transfer (CT) absorption bands in the near-ultraviolet (nUV) and effective f–f transition of Eu^{3+}.[12-15] White LEDs can offer benefits in terms of high luminous efficiency, maintenance, and environmental protection.[16-18] To obtain a higher efficiency white LED with an appropriate color temperature and a higher color-rendering index, a new approach using nUV InGaN-based LED chip coated with blue/green/red tricolor phosphors was introduced.[19] However, the lack of effective red phosphor blocks the development of white LEDs because few red phosphors could be excited efficiently by blue or nUV light. Therefore, it is of high interest to search for a suitable red phosphor for the fabrication of LEDs. However, among the previously published results, nearly all of the molybdates were synthesized by the conventional solid-state reaction method or sol–gel method with further calcination treatment ($\geq$700°C).[20-23] These approaches usually require high temperatures, time-consuming heating processes, and subsequent grinding. The grinding process damages the phosphor surfaces, resulting in the loss of emission intensity.[24,25] The aggregation and inhomogeneous shape are also unavoidable, which inhibit the absorption of the excitation energy and therefore reduce the emission intensity. Therefore, a simple and economical method for making high quality phosphors is desirable.

Recently, the template-free hydrothermal method has been considered as a good synthesis process for some inorganic powders because of the available synthesis of crystallized products at low reaction temperature, flexibility in the design of reaction conditions, uniformity of product composition, phase, and microstructure, and simplicity of the equipment and processing.[26] In this paper, we reported that the octahedral $NaGd(MoO_4)_2:Eu^{3+}$ microcrystals were synthesized by a facile one-step hydrothermal process without using any templates, surfactant, other organic additives, and further calcination treatment. The optimal synthesized conditions for $NaGd(MoO_4)_2:Eu^{3+}$ microcrystals were studied. A phenomenological growth mechanism for the octahedron microcrystals has been proposed. Finally, the luminescent properties of the $NaGd(MoO_4)_2:Eu^{3+}$ microcrystals were also presented, which showed an intensive red emission, indicating that the $NaGd(MoO_4)_2:Eu^{3+}$ microcrystals may become potential excellent red phosphors for white LEDs.

Experimental

Preparation of $NaGd(MoO_4)_2:Eu^{3+}$ microcrystals.— Materials.— All reagents from Beijing Chemical Co. were analytical grade and used directly without further purification. Ammonium molybdate tetrahydrate $[(NH_4)_6Mo_7O_{24}\cdot 4H_2O]$ was used as the molybdenum source, gadolinium nitrate hexahydrate $[Gd(NO_3)_3\cdot 6H_2O]$ as the gadolinium source, sodium hydroxide (NaOH) as the sodium source, and europium nitrate pentahydrate $[Eu(NO_3)_3\cdot 5H_2O]$ as the europium source. For the hydrothermal treatment, we used 60 mL Teflon cups.

Synthesis.— Appropriate amounts of $(NH_4)_6Mo_7O_{24}\cdot 4H_2O$, $Gd(NO_3)_3\cdot 6H_2O$, and $Eu(NO_3)_3\cdot 5H_2O$ were dissolved in 35 mL distilled water to form aqueous solutions and then mixed together with strong magnetic stirring at room temperature for 10 min to form a homogeneous solution. Next, the same solutions were adjusted to pH 4.5, 5, 5.5, 6, and 7 by adding dropwise into the above solutions with a desired amount of NaOH (5 M) under vigorous stirring before hydrothermal treatment. The amount of NaOH was controlled by the pH value shown on the pH meter (the microdigit

[z] E-mail: zlfu@jlu.edu.cn; dai@jlu.edu.cn

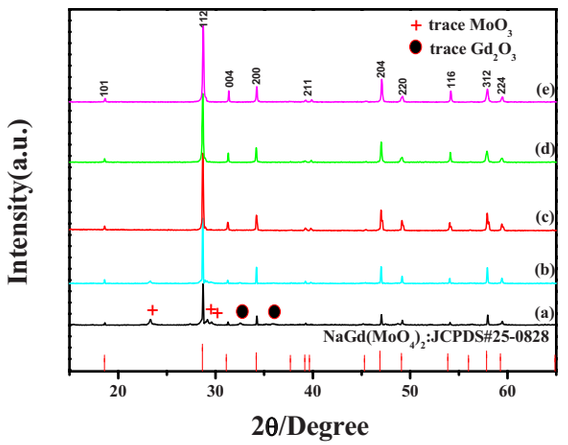

Figure 1. (Color online) XRD powder patterns of $NaGd(MoO_4)_2:Eu^{3+}$ samples prepared by hydrothermal method at 180°C for 12 h at pH (a) 4.5, (b) 5, (c) 5.5, (d) 6, and (e) 7.

pH/mv meter with a high accuracy of ±0.01 pH), and was assisted with the diluted HNO_3 solution by adding it dropwise when necessary. First, NaOH immediately reacted with the molybdenum source and rare-earth nitrate solutions, and a slurrylike white precipitate was formed. The mixture was stirred again for 1 h. Finally, the mixture was placed in a poly(tetrafluoroethylene) (PTFE) vessel, and the vessel was capped by a PTFE cover and placed inside a stainless steel autoclave. The autoclave was maintained at 180°C for 12 h and cooled naturally to room temperature. The precipitate was filtered and washed with alcohol and deionized water several times. The precipitates were dried at 60°C on air. Finally, the uniform distribution of octahedral $NaGd(MoO_4)_2:Eu^{3+}$ microcrystals were obtained. To investigate the intermediates of the octahedral $NaGd(MoO_4)_2:Eu^{3+}$, the synthesis was stopped at different stages during the synthesis process. In addition, the activator content (Eu) was maintained at 4 mol % for the prepared samples.

Characterization.— Powder X-ray diffraction (XRD) measurements were performed on a Rigaku D/max 2500 diffractometer with Cu Kα radiation (λ = 0.15405 nm). The morphology and structure of the obtained samples were inspected using a field-emission-scanning electron microscope (FESEM, XL30, Philips). The UV-visible PL excitation and emission spectra were recorded with a Hitachi F-7000 spectrophotometer equipped with a Xe lamp as an excitation source. All the measurements were performed at room temperature.

Results and Discussion

Synthesis and morphology of $NaGd(MoO_4)_2:Eu^{3+}$.— Figure 1 shows the results of the XRD analysis of the hydrothermal reaction products obtained at 180°C for 12 h under different pH values. The suitable pH value for the synthesis of single-phase crystalline $NaGd(MoO_4)_2:Eu^{3+}$ powders was investigated by varying the base (NaOH) concentration used in the reaction system. At pH ≤ 5, a trace of Gd_2O_3 and MoO_3 appeared as impurity [pH 4.5 (Fig. 1a) and pH 5 (Fig. 1b)], whereas beginning at pH 5.5, no impurity peaks were detected in this experimental range (Fig. 1c). All of the diffraction peaks can be indexed to the Scheelite-type tetragonal structure (JCPDS no. 25-0828) with the $I4_1/a$ lattice symmetry. The lattice constants are calculated to be $a = b = 5.237$ Å and $c = 11.437$ Å. When the pH value varied from 6 to 7, we can also obtain the pure phase [pH 6 (Fig. 1d) and pH 7 (Fig. 1e)]. Therefore, NaOH reacted with Gd^{3+} and MoO_4^{2-} properly beginning at pH 5.5.

To fully understand the effect of pH value on the microstructure and morphology of the synthesized samples, controlled experiments were conducted to find the optimal morphology. Figure 2 shows the

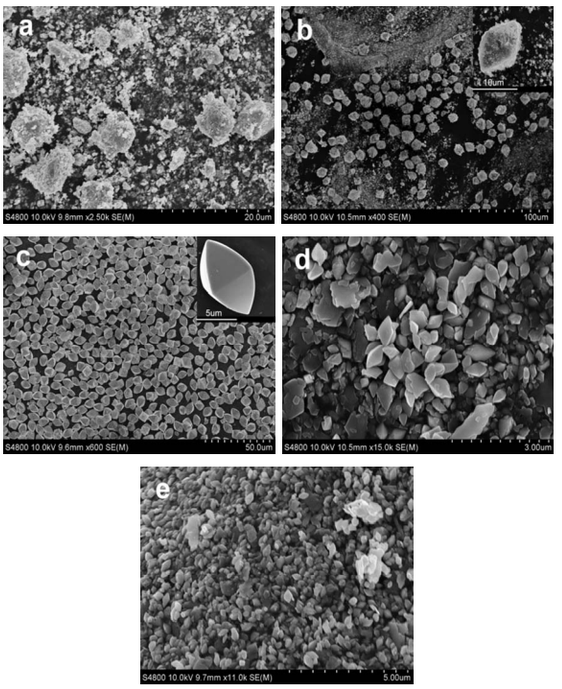

Figure 2. FESEM images of $NaGd(MoO_4)_2:Eu^{3+}$ crystallites prepared hydrothermally at 180°C for 12 h at pH (a) 4.5, (b) 5, (c) 5.5, (d) 6, and (e) 7. Insets in (b) and (c) show the FESEM images of randomly selected particle of $NaGd(MoO_4)_2:Eu^{3+}$ microcrystals.

morphology evolution of resultant $NaGd(MoO_4)_2:Eu^{3+}$ crystallites from different starting pH values after hydrothermal treatment at 180°C for 12 h. Obviously, the morphology of $NaGd(MoO_4)_2:Eu^{3+}$ crystallites can be tailored by adjusting the pH value of the suspension solution. At pH 4.5 (Fig. 2a), the micrographs revealed the presence of $NaGd(MoO_4)_2:Eu^{3+}$ powders with some agglomerate and small seeds, presenting a polydisperse nature. Some octahedron-like microparticles with small seeds appeared at pH 5 (Fig. 2b). By increasing the pH value to 5.5 (Fig. 2c), the uniform octahedral $NaGd(MoO_4)_2:Eu^{3+}$ microcrystals in good dispersancy and with a diameter of ~5 μm were obtained, and the magnified view shows that these crystals are regular octahedra and have smooth faces. When the pH value varied from 6 to 7 (Fig. 2d and e), octahedral microcrystals disappeared and different polyhedral morphologies of $NaGd(MoO_4)_2:Eu^{3+}$ appeared.

On the basis of the above discussion, our experimental results indicated that the starting pH value played an important role in the pure-phase formation and uniform morphology of octahedral $NaGd(MoO_4)_2:Eu^{3+}$ microcrystals. The crystalline phase of the nuclei is critical for directing the intrinsic shapes of the crystals due to its characteristic symmetry and structure.[27] NaOH acting as the mineralizer in varying the pH value, to a certain extent, would change the growth rate of crystallographic planes with different surface energies so as to form different crystallite morphologies.[28-33] Therefore, a crystallization pH value of 5.5 was optimal.

Formation mechanism for the octahedral $NaGd(MoO_4)_2:Eu^{3+}$ microcrystals.— The crystal growth mechanisms in the solution are so complicated that the actual crystallization mechanism remains an open question. Considering that there are no additional templates and surfactants in the present case, it is reasonable that the growth and formation of the microstructure is neither catalyst- nor template-assisted because the only source materials used in this case are pure $(NH_4)_6Mo_7O_{24}{\cdot}4H_2O$, $Gd(NO_3)_3$, and NaOH. On the basis of time-dependent experiments (FESEM in Fig. 3), octahedral

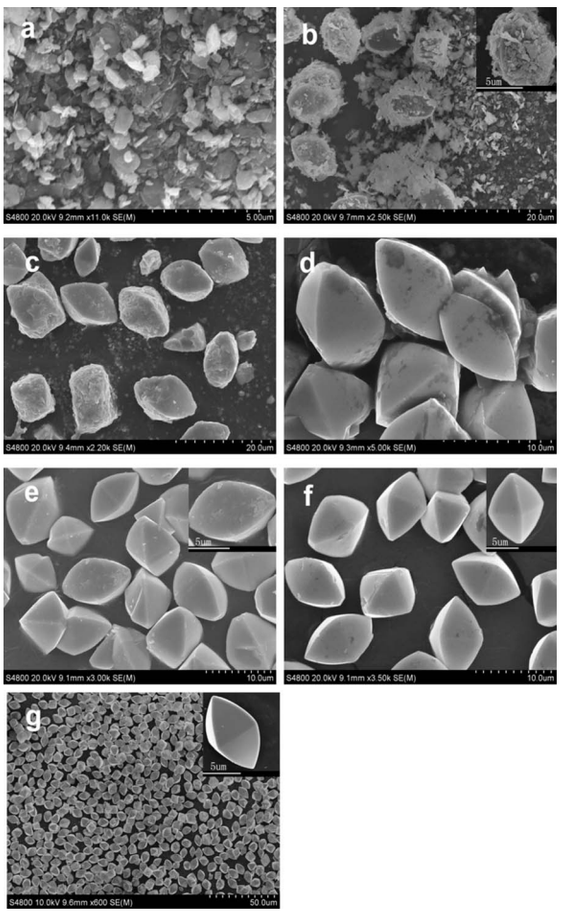

Figure 3. FESEM images of the products synthesized at 180°C and pH 5.5 with different hydrothermal reaction times: (a) 0, (b) 2, (c) 4, (d) 6, (e) 8, (f) 10, and (g) 12 h.

$NaGd(MoO_4)_2$:Eu^{3+} microcrystals can be obtained via a nucleation–crystallization-oriented attachment growth mechanism. The kinetically controlled oriented attachment growth process was also observed by Penn and Banfield[34] and Jun et al.[35] in the synthesis of the TiO_2 nanostructure.

For better understanding of the formation process of the octahedral $NaGd(MoO_4)_2$:Eu^{3+} microcrystals, reaction products obtained at different growth stages were carefully examined by FESEM observations. Before the hydrothermal reaction, tiny microparticles and seeds (Fig. 3a) were formed after the precipitate was stirred for 1 h. Once the $NaGd(MoO_4)_2$ nuclei were formed, new reactants continuously arrived at the site. Figure 3b showed the morphology of the products synthesized at 180°C for 2 h under hydrothermal conditions. We got some accumulated octahedron-like nucleation, which were composed of some tiny microparticles and seeds. When the reaction time was increased to 4 h, the octahedron-like nucleation acted as the centers of crystallization; the crystal growth then followed, and bigger particles grew at the expense of small crystals, which are shown in Fig. 3c. As the reaction proceeded, the crystals with the accidental surface were further grown on the basis of octahedron-like microcrystals, which could be thought of as the framework of an octahedron (Fig. 3d). Upon continuing the reaction, the surface of the octahedron-like microcrystals became smooth (Fig. 3e and f). Finally, the perfect octahedral $NaGd(MoO_4)_2$:Eu^{3+} microcrystals were obtained (Fig. 3g).

It is believed that the reduction in surface energy is the primary driving force for simple particle growth; the further reduction in surface energy due to the minimization of high surface energy faces drives the morphology evolution. From the crystal growth point of view, the shape of the crystal highly depends on the relative growth rates of various crystal planes.[36] Generally, the surface energy of the {100} crystal face is higher than that of the {111} face, which causes the growth rate along the ⟨100⟩ direction to be faster than those along the ⟨111⟩ direction.[37] Therefore, the growth rate of the {100} surface is faster than that of the {111} surface, and then the fast-growing {100} faces eventually disappeared during the growth, resulting in the formation of truncated octahedron microcrystals (Fig. 3f). Due to the lower disappearing rate of the {001} faces, the prime bipyramidal octahedra with a longer axis were obtained (Fig. 3g). From the above analysis, the nucleation–crystallization-oriented attachment growth process contains obvious evolution stages for the synthesis of octahedral $NaGd(MoO_4)_2$:Eu^{3+} microcrystals. The process of the morphology evolution of octahedral $NaGd(MoO_4)_2$:Eu^{3+} microcrystals is schematically illustrated in Scheme 1.

Luminescent properties.— Eu^{3+} ion is a well-known red-emitting activator in commercial phosphors because the emission of the rare-earth Eu^{3+} ion consists usually of lines in the red spectral area and these lines from the $^5D_0 - {}^7F_J$ (J = 1, 2, 3, 4, 5, and 6) transitions. Moreover, Eu^{3+}-doped phosphors usually have effective and intrinsic absorption due to the 4f–4f transition of Eu^{3+} at ~395 or 465 nm, which makes it well-matched with the blue/nUV LED chips as an efficient red light emitting phosphor. Figure 4 shows the PL excitation and emission spectra of the $NaGd(MoO_4)_2$:Eu^{3+} phosphor with different morphologies, arising from different starting pH values. The excitation spectra (Fig. 4, left) were obtained by monitoring the emission of the Eu^{3+} $^5D_0 - {}^7F_2$ transition at 616 nm. The excitation spectrum consists of a strong and broad band from 200 to 350 nm with a maximum at ~285 nm, which is ascribed to the O–Mo CT transition.[38] In the longer wavelength region (360–500 nm), the sharp lines are intraconfigurational 4f–4f transitions of Eu^{3+} in the host lattices, and the strong excitation band at 395 and 466 nm is attributed to the $^7F_0 - {}^5L_6$ and $^7F_0 - {}^5D_2$ transitions of Eu^{3+}, re-

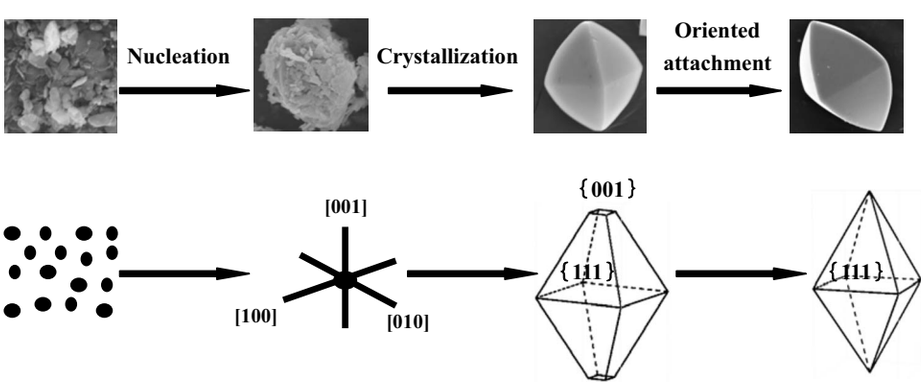

Scheme 1. Schematic illustration of the formation and morphology evolution of octahedral $NaGd(MoO_4)_2$:Eu^{3+} microcrystals in the whole synthetic process.

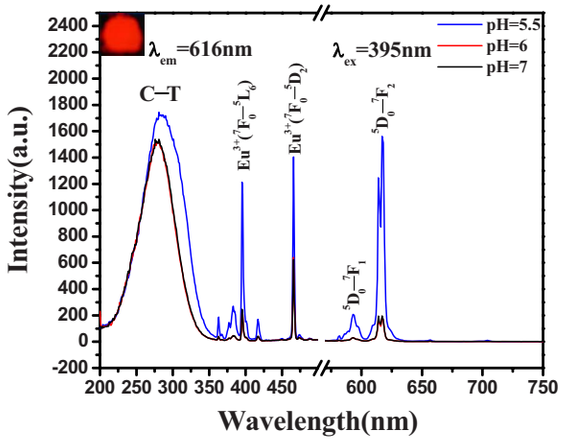

Figure 4. (Color online) PL excitation and emission spectra of $NaGd(MoO_4)_2:Eu^{3+}$ microcrystals prepared hydrothermally at 180°C for 12 h from different starting pH values. Corresponding luminescence photograph for sample under excitation of 254 nm UV lamp irradiation in dark.

spectively. Upon UV excitation at 395 nm, the $NaGd(MoO_4)_2:Eu^{3+}$ samples exhibit a strong red luminescence. The emission spectra are described by the well-known $^5D_0 - {}^7F_J$ (J = 1,2) emission lines of the Eu^{3+} ions with the strong emission for J = 2 at 616 nm, and the sample displays a bright red color to the naked eye (inset of Fig. 4). It indicates that Eu^{3+} occupies a center of asymmetry in the host lattice. The transition $^5D_0 - {}^7F_2$ is much stronger than the transition $^5D_0 - {}^7F_1$, which is favorable to improve the color purity of the red phosphor. In addition, from the emission spectra (Fig. 4, right), the PL intensity of octahedral $NaGd(MoO_4)_2:Eu^{3+}$ microcrystals in good morphology prepared from pH 5.5 is the strongest, and about 8 times stronger than the other samples (pH 6 and 7). In summary, uniform and well-crystallized octahedral $NaGd(MoO_4)_2:Eu^{3+}$ microcrystals synthesized in our experiment showed an intensive red emission, indicating that it may be applied as an excellent red component for nUV white LEDs.

Conclusion

In summary, a simple one-step hydrothermal method has been successfully used to grow well-crystallized octahedral $NaGd(MoO_4)_2:Eu^{3+}$ microcrystals without using any templates, surfactant, and other organic additives. Crystallization pH 5.5 was optimal for the pure-phase synthesis and uniform morphology of $NaGd(MoO_4)_2:Eu^{3+}$ octahedron microcrystals. The formation process of the octahedron was investigated in detail by time-dependent experiments. The as-synthesized $NaGd(MoO_4)_2:Eu^{3+}$ microcrystals prepared at pH 5.5 show the strongest red emission centered at ~616 nm from Eu^{3+} under UV excitation, which may have potential application for white LEDs. Further work is underway to study the intrinsic physical property of the well-prepared samples and the possibility of synthesizing other related materials.

Acknowledgments

This work was supported by the Fundamental Research Funds for the Central Universities (no. 421060551411), partially supported by a grant-in-aid for the National Science Foundation of China (no. 10974066), and by the Program for New Century Excellent Talents in University (no. NCET-05-0302, China).

References

1. D. D. Archibald and S. Mann, *Nature (London)*, **364**, 430 (1993).
2. A. P. Alivisatos, *Science*, **271**, 933 (1996).
3. Z. H. Xu, C. X. Li, P. P. Yang, C. M. Zhang, S. S. Huang, and J. Lin, *Cryst. Growth Des.*, **9**, 4752 (2009).
4. X. D. Wang, J. H. Song, J. Liu, and Z. L. Wang, *Science*, **316**, 102 (2007).
5. S. J. Chen, Y. C. Liu, C. L. Shao, R. Mu, Y. M. Lu, J. Y. Zhang, D. Z. Shen, and X. W. Fan, *Adv. Mater.*, **17**, 586 (2005).
6. L. Zhang, D. R. Chen, and X. L. Jiao, *J. Phys. Chem. B*, **110**, 2668 (2006).
7. J. Yang, Z. W. Quan, D. Y. Kong, X. M. Liu, and J. Lin, *Cryst. Growth Des.*, **7**, 730 (2007).
8. B. Mikhailik, H. Kraus, M. Itoh, D. Iri, and M. Uchida, *J. Phys.: Condens. Matter*, **17**, 7209 (2005).
9. J. L. Brito and A. L. Barbosa, *J. Catal.*, **171**, 467 (1997).
10. A. Kaddouri, R. D. Rosso, C. Mazzocchia, P. Gronchi, and D. Fumagalli, *J. Therm Anal. Calorim.*, **66**, 63 (2001).
11. B. Mikhailik, B. Kraus, D. Wahl, and M. S. Mykhaylyk, *Phys. Status Solidi B*, **242**, R17 (2005).
12. C. F. Guo, W. Zhang, L. Luan, T. Chen, H. Cheng, and D. X. Huang, *Sens. Actuators B*, **133**, 33 (2008).
13. S. Neeraj, N. Kijima, and A. K. Cheetham, *Chem. Phys. Lett.*, **387**, 2 (2004).
14. Z. L. Wang, H. B. Liang, J. Wang, M. L. Gong, and Q. Su, *Appl. Phys. Lett.*, **89**, 071921 (2006).
15. S. K. Shi, J. Gao, and J. Zhou, *J. Electrochem. Soc.*, **155**, H525 (2008).
16. Z. L. Wang, H. B. Liang, L. Y. Zhou, H. Wu, M. L. Gong, and Q. Su, *Chem. Phys. Lett.*, **412**, 313 (2005).
17. S. Yan, J. Zhang, X. Zhang, S. Lu, X. Ren, Z. Nie, and X. Wang, *J. Phys. Chem. C*, **111**, 13256 (2007).
18. J. G. Wang, X. P. Jing, C. H. Yan, and J. H. Lin, *J. Electrochem. Soc.*, **152**, G186 (2005).
19. J. K. Sheu, S. J. Chang, C. H. Kuo, Y. K. Su, L. W. Wu, Y. C. Lin, W. C. Lai, J. M. Tsai, G. C. Chi, and R. K. Wu, *IEEE Photon. Technol. Lett.*, **15**, 18 (2003).
20. L. Y. Zhou, L. H. Yi, R. F. Sun, F. Z. Gong, and J. H. Sun, *J. Am. Ceram. Soc.*, **91**, 3416 (2008).
21. C. F. Guo, S. T. Wang, T. Chen, L. Luan, and Y. Xu, *Appl. Phys. A: Mater. Sci. Process.*, **94**, 365 (2009).
22. C. P. Grey, C. M. Dobson, A. K. Cheetham, and R. J. B. Jakeman, *J. Am. Chem. Soc.*, **111**, 505 (1989).
23. B. J. Kennedy, B. A. Hunter, and C. J. Howard, *J. Solid State Chem.*, **130**, 58 (1997).
24. D. Boyer, G. Bertrand-Chadeyron, R. Mahiou, C. Caperaa, and J.-C. Cousseins, *J. Mater. Chem.*, **9**, 211 (1999).
25. M. K. Jung, W. J. Park, and D. H. Yoon, *Sens. Actuators B*, **126**, 328 (2007).
26. H. M. Cheng, J. M. Ma, Z. G. Zhao, and L. M. Qi, *Chem. Mater.*, **7**, 663 (1995).
27. D. Chen, K. B. Tang, F. Q. Li, and H. G. Zheng, *Cryst. Growth Des.*, **6**, 247 (2006).
28. S. H. Yu, B. Liu, M. S. Mo, J. H. Huang, X. M. Liu, and Y. T. Qian, *Adv. Funct. Mater.*, **13**, 639 (2003).
29. C. Jia, Y. Cheng, F. Bao, D. Q. Chen, and Y. S. Wang, *J. Cryst. Growth*, **294**, 353 (2006).
30. H. Wu, H. F. Xu, Q. Su, T. H. Chen, and M. M. Wu, *J. Mater. Chem.*, **13**, 1223 (2003).
31. B. Liu, S. H. Yu, L. J. Li, Q. Zhang, F. Zhang, and K. Jiang, *Angew. Chem., Int. Ed.*, **43**, 4745 (2004).
32. Y. W. Jun, J. H. Lee, J. S. Choi, and J. Cheon, *J. Phys. Chem. B*, **109**, 14795 (2005).
33. X. M. Wang, H. Y. Xu, H. Wang, and H. Yan, *J. Cryst. Growth*, **284**, 254 (2005).
34. R. L. Penn and J. F. Banfield, *Am. Mineral.*, **83**, 1077 (1998).
35. Y. Jun, M. F. Casula, J. H. Sim, S. Y. Kim, J. Cheon, and A. P. Alivisatos, *J. Am. Chem. Soc.*, **125**, 15981 (2003).
36. D. Yuvaraj, K. Narasimha Rao, and K. Barai, *Solid State Commun.*, **149**, 349 (2009).
37. Z. L. Wang, *J. Phys. Chem. B*, **104**, 1153 (2000).
38. J. A. Groenink, C. Hakfoort, and G. Blasse, *Phys. Status Solidi A*, **54**, 329 (1979).